Ion cyclotron emission and the nonlinear physics of the magnetoacoustic cyclotron instability of fusion-born ions

L Carbajal[1], R O Dendy[2,1], S C Chapman[1] and J W S Cook[1]

[1]*Centre for Fusion, Space and Astrophysics, Department of Physics, Warwick University, Coventry CV4 7AL, U.K.*

[2]*CCFE, Culham Science Centre, Abingdon, Oxfordshire OX14 3DB, U.K.*

1. Introduction

Ion cyclotron emission (ICE)[1] was the first collective radiative instability, driven by fusion products, that was observed from deuterium-tritium plasmas in both JET[1-4] and TFTR[5]. Intensely suprathermal emission, strongly peaked at the frequencies of sequential ion cyclotron harmonics as evaluated at the outer mid-plane edge, was detected using heating antennas in receiver mode on JET and using probes in TFTR. The measured intensity of ICE spectral peaks scaled linearly with measured fusion reactivity. Linear analytical theory together with particle orbit calculations early suggested that the emission mechanism is the magnetoacoustic cyclotron instability (MCI)[6,7], driven by a subset of centrally born fusion products, lying just inside the trapped-passing boundary in velocity space, whose drift orbits make large radial excursions[2,5] to the outer mid-plane edge in both tokamaks. More recently, in other large tokamak plasmas, ICE has been used as a diagnostic for lost fast ions in DIII-D[8], and has been studied in detail in ASDEX-U[9] and JT-60U[10]. ICE is a potential diagnostic for alpha-particles in ITER[11], and it may also be possible to use ICE to study fast ion redistribution and loss due to MHD activity in ITER. For example, clear evidence has been found of links between ICE and sawteeth[12] and ELMs[2] in JET, fishbones[8] in DIII-D, and TAEs[13] in LHD. Deep understanding of the MCI is therefore of great practical interest for magnetic confinement fusion, and advances in computational plasma physics have led to substantial recent progress. Recent large scale particle-in-cell (PIC) simulations of the MCI extending into its nonlinear regime[14], with fully kinetic ions and electrons and using plasma parameters aligned to relevant JET conditions, strengthened the link to observations. Subsequent simulations of the MCI over even longer physical time durations[15] used the hybrid approximation, where ions are treated as particles and electrons as a neutralising massless fluid. These simulations[14,15] corroborate predictions by linear analytical theory and, by extending previous studies deep into the nonlinear regime of the MCI, appear to confirm that the MCI underlies the ICE observations.

2. Hybrid simulation model

The hybrid model treats ions as kinetic particles, whose positions evolve continuously in physical and velocity space, each acted upon by the local Lorentz force. The magnetic field is updated using Faraday's law, and the electric field using the electron fluid momentum equation in the limit of zero electron inertia[15,16]. Like PIC models, hybrid models resolve ion kinetics, including gyromotion. This enables the study of instabilities that evolve fast[17], unfolding on timescales rapid compared to gyro-averaged or fluid phenomena, and very rapid compared to collisional slowing-down. In the simulations[14,15] reviewed here, the majority thermal plasma is supplemented by an energetic minority alpha-particle population, whose concentration relative to the thermal ions is $\xi = 10^{-3}$ to 10^{-4}. In velocity space this population is represented by a ring-beam with characteristic energy 3.5MeV.

3. Results

Figure 1, reproduced from [15], compares an observed ICE spectrum from a JET deuterium-tritium plasma with the outputs of MCI studies in two categories: linear analysis, and hybrid simulations. A consistent picture emerges: agreement is good, and increases with the run-time of the simulations, as seen in the bottom panel.

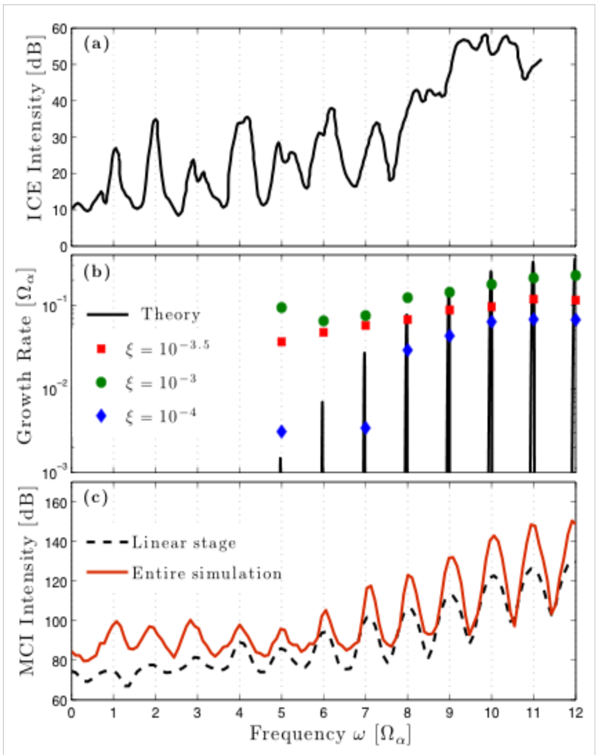

Fig.1, reproduced from Ref.[15]. Experimental ICE spectra compared with spectra obtained from MCI studies. Top panel: Measured ICE intensity from JET deuterium-tritium plasma 26148. Middle panel: Analytical linear growth rate for the MCI for the number density ratio $\xi = 10^{-3}$, along with the early time (linear) growth rate of the MCI inferred from the hybrid simulations for the three values, $\xi = 10^{-3}$, $10^{-3.5}$, 10^{-4}. Bottom panel: Intensity of the electromagnetic field component B_z of the hybrid simulation with number density ratio $\xi = 10^{-3}$. The dashed black (solid red) line represents the linear (nonlinear) stage of the instability.

The hybrid model follows the MCI deep into its nonlinear phase, which enables this treatment[15] to capture additional aspects of the observed ICE signal. Comparison of the two traces for the simulated MCI in Fig.1(bottom) with the measured ICE signal in Fig.1(top) shows that only the solid red trace, which encompasses the nonlinear phase, captures the lower observed cyclotron harmonic peaks one to three. These appear to reflect stronger drive at low cyclotron harmonics due to nonlinear coupling between low and high frequency modes of the electromagnetic field that are excited in the early phase. This is shown in Fig.2, which shows bicoherence plots at early and late times.

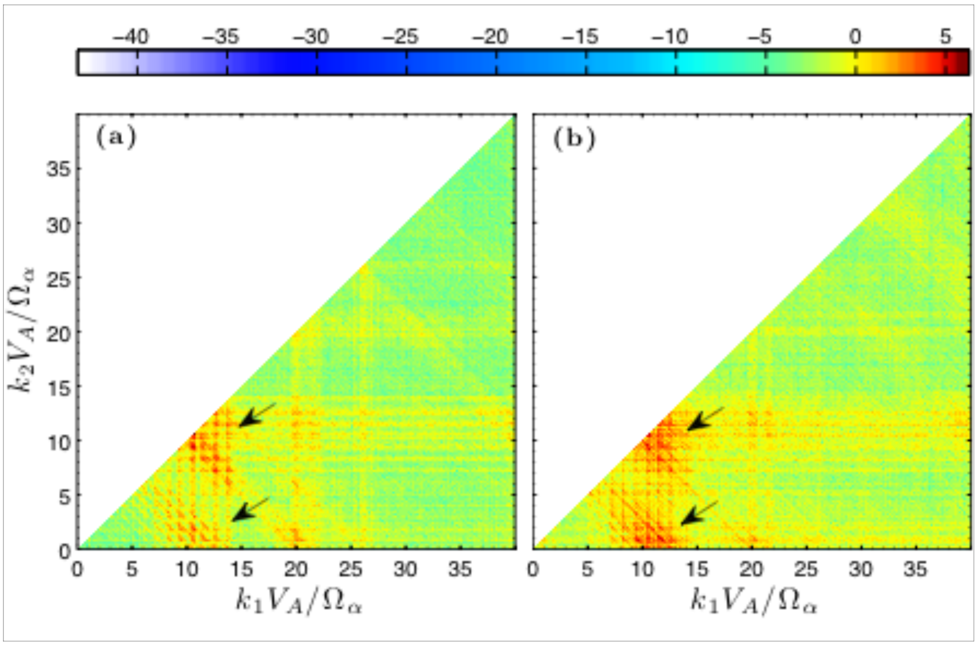

Fig.2, reproduced from Ref.[15]. Origin of strong spectral peaks at the lowest cyclotron harmonics. The non-normalized self-bicoherence of the B_z component in wavenumber space is plotted using a $\log_{10}$ colour scale. Only the principal domain of the self-bicoherence is shown. The red colour indicates significant coupling between different modes at k_1 and k_2. Lefty and right panels show the non-normalised self-bicoherence of B_z in the linear and nonlinear stages of the MCI, respectively. The arrows in both panels point to areas in the (k_1, k_2) plane where strong coupling occurs between low and high wavenumbers, which correspond to cyclotron harmonic numbers ω/Ω_α in the ranges 1-3 and 9-12, respectively.

Our results for the nonlinear stage of the MCI show other novel features[15]. Interestingly, for example, the alpha-particle population can become re-energised through transit-time compressional magnetic pumping, driven by electromagnetic modes excited by these alpha-particles in the earlier stage of the MCI.

4. Conclusions

It is very probable that the plasma physics process underlying ICE is the MCI. This was strongly suggested by the original linear analytical theory approach to ICE from deuterium-tritium plasmas in JET and TFTR[1-7]. It appears to be confirmed by the large scale numerical simulations using PIC and hybrid codes[14,15] reviewed here. This depth of understanding of the emission mechanism is essential if ICE is to be exploited as a diagnostic of confined and lost fusion alpha-particles in ITER, as has been proposed[11]. Our simulations indicate that most of the key physics unfolds on the rapid timescale of a few cyclotron periods, which is short compared to the evolution timescale of the overall alpha-particle population in quasi-steady state.

These results may have applications beyond fusion plasma physics. In space, phenomenology similar to ICE has been observed in terrestrial magnetospheric plasmas under conditions where it is likely to be driven by the MCI[18,19]. In astrophysics, the possibility of related effects at supernova remnant (SNR) shocks was originally noted in [20]. Subsequent simulations showed that waves excited by the MCI under SNR conditions are capable of accelerating ambient background electrons to mildly relativistic energies[21,22]. Recent PIC simulations show the concentration of wave energy in sequential ion cyclotron harmonic peaks[23] in the region downstream of SNR shocks. ICE and the MCI also pose a fundamental question in classical electrodynamics: if we create a minority drifting ring-beam population of energetic ions in a plasma, how do this population, the plasma, and the self-consistently excited fields evolve and interact over the long term?

LC acknowledges the Mexican Council of Science and Technology (CONACyT) for support. This work was part-funded by the RCUK Energy Programme and by the European Union's Horizon 2020 programme.

[1] G A Cottrell and R O Dendy, Phys. Rev. Lett. **60** 33 (1988)
[2] G A Cottrell, V P Bhatnagar *et al.*, Nucl. Fusion **33** 1365 (1993)
[3] R O Dendy, K G McClements *et al.*, Nucl. Fusion **35** 1733 (1995)
[4] K G McClements, C Hunt *et al*., Phys. Rev. Lett. **82** 2099 (1999)
[5] S Cauffman, R Majeski *et al*., Nucl. Fusion **35** 1597 (1995)
[6] R O Dendy, K G McClements *et al*., Phys. Plasmas **1** 1918 (1994)
[7] K G McClements, R O Dendy *et al*., Phys. Plasmas **3** 543 (1996)
[8] W W Heidbrink *et al*., Plasma Phys. Control. Fusion **53** 085028 (2011)
[9] R D'Inca, M Garcia-Munoz *et al*., Proc. 38th EPS Conf. Plasma Phys. 2012 P1.053
[10] M Ichimura, H Higaki *et al*., Nucl. Fusion **48** 035012 (2008)
[11] K G McClements, R O Dendy *et al*., IAEA Fusion Energy Conf., submitted (2014)
[12] P Schild, G A Cottrell, and R O Dendy, Nucl. Fusion **29** 834 (1989)
[13] K Saito, R Kumazawa *et al*., Plasma Sci. Technol. **15** 209 (2013)
[14] J W S Cook, R O Dendy *et al*., Plasma Phys. Control. Fusion **55** 065003 (2013)
[15] L Carbajal, R O Dendy, S C Chapman *et al*., Phys. Plasmas **21** 012106 (2014)
[16] P W Gingell, S C Chapman et al., Plasma Phys. Control. Fusion **54** 065005 (2012)
[17] W W Heidbrink and G Sadler, Nucl. Fusion **34** 535 (1994)
[18] K G McClements and R O Dendy, J. Geophys. Res. **98** 11689 (1993)
[19] R O Dendy and K G McClements, J. Geophys. Res. **98** 15531 (1993)
[20] K G McClements, R O Dendy *et al*., Mon. Not. R. Astr. Soc. **280** 219 (1996)
[21] M E Dieckmann, K G McClements *et al*., Astron. Astrophys. **356** 377 (2000)
[22] H Schmitz, S C Chapman and R O Dendy, Astrophys. J. **579** 327 (2002)
[23] V L Rekaa, S C Chapman and R O Dendy, Astrophys. J, submitted (2014)